An Analysis of Galileo E5 Signal Acquisition Strategies

Nagaraj C Shivaramaiah, Andrew G Dempster,
University of New South Wales, Sydney, Australia

BIOGRAPHY

Nagaraj C Shivaramaiah is currently a doctoral student within the GNSS receiver design group in the School of Surveying and Spatial Information Systems at the University of New South Wales, Australia. He obtained his Masters degree from the Centre for Electronics Design and Technology at Indian Institute of Science, Bangalore, India. His research interests include base band signal processing and FPGA based receiver design for GNSS.

Andrew G Dempster is the Director of Research in the School of Surveying and Spatial Information Systems at the University of New South Wales. He led the team that developed Australia's first GPS receiver in the late 80s and has been involved with satellite navigation ever since. His current research interests are GNSS receiver design, GNSS signal processing, and new location technologies.

INTRODUCTION

In Global Navigation Satellite System (GNSS) acquisition, Probability of Detection P_d and Mean Acquisition Time $\overline{T_{acq}}$ have a direct and inverse relation to the signal to noise ratio of the desired signal respectively. The code length and the auto-correlation properties of the ranging code, granularity of time and frequency steps and the search strategy all influence the P_d and $\overline{T_{acq}}$ for a specified Probability of False Alarm (P_{fa}). BPSK modulated ranging codes employed by GPS offer a single peak triangular auto-correlation function (ACF) which in most situations provides a good *Pd* and $\overline{T_{acq}}$ for half-chip search steps. However, Binary-Offset-Carrier (BOC) modulations employed in new GNSS signals produce multiple peaks in the ACF which create ambiguities during acquisition and require better processing to achieve P_d and $\overline{T_{acq}}$ comparable to that of GPS L1 under similar conditions. Galileo E5 signals demand additional computation due to the signal structure where four codes are combined using Alternate-Binary-Offset-Carrier (AltBOC) modulation.

Several techniques have been proposed in the literature to efficiently achieve the required P_d and $\overline{T_{acq}}$. These can be broadly classified as search strategy based and correlation scheme based techniques. Some of the former techniques are mentioned in [1] and the latter in [2, 3]. Search strategy based techniques generally address the $\overline{T_{acq}}$. For example, by correlating the two side-bands independently, acquisition engines can operate at a lower sampling frequency and can increase the code search step size. Correlation scheme based techniques (viz. BPSK-like methods) generally tackle the ambiguity problem by modifying the correlation triangle and hence increasing the P_d . This paper analyses the P_d and $\overline{T_{acq}}$ for the methods that are used in these two techniques.

First, the effect of code search step size on the auto-correlation value is analysed for AltBOC(15,10) modulation. It is seen that the worst-case (at the corresponding residual code phase offset) correlation plot has nulls which affect the P_d . Next, the correlation plots and code search step size effects for the aforementioned acquisition techniques are analysed and P_d and $\overline{T_{acq}}$ are compared. It is noted that the $|VE^2+P^2|$ method mentioned in [2] is a special case of a more generalized method given by [4] with the delayed addition equivalent to one quarter of the ratio of the sub-carrier period to the chip period. When applied to AltBOC(15,10) modulation with 0.167chips (ideal case, although this depends on the receiver front-end bandwidth) as the delay parameter in this method, P_d and $\overline{T_{acq}}$ are comparable to the BPSK-like methods. This enables the acquisition engine to search at larger chip steps (up to 0.8 chips) by employing a search strategy with disjoint addition of the successive samples. Finally it is shown that the implementation can be achieved with just a second arm out of the local AltBOC(15,10) replica generator look-up table, without having to shift all the four codes.

E5 SIGNAL STRUCTURE AND THE CORRELATION FUNCTION

Unlike its counterparts, the Galileo E5 signal employs a complex sub-carrier modulation known as AltBOC(15,10) modulation. The sub-carriers are specially chosen waveforms that result in a split spectrum and a constant envelope after the modulation. Four codes are combined with these specially chosen complex sub-

carriers to obtain the modulating signal which then phase modulates the E5 carrier. Alternatively, the complete modulation can be seen as an 8-PSK modulation [5, 6, 7]. The spectrum is shown in Figure 1. Note that the transmitted signal occupies a bandwidth of 51.15MHz to cover the two main lobes, giving E5 the largest bandwidth of any GNSS signal.

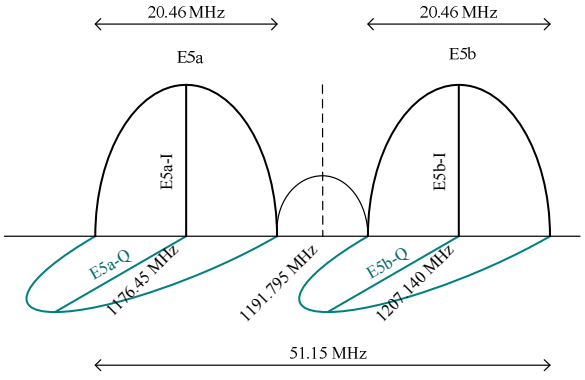

Figure 1 E5 Signal Spectrum

A direct method to process the E5 signal at the receiver is to receive the signal in the entire 51.15MHz bandwidth and perform the correlation with the locally generated replica of the modulating signal. This results in a correlation function as shown in Figure 2. Observe that the shape of the correlation waveform is similar to a BOC(10,15) signal and possesses side peaks along with a sharp main correlation triangle.

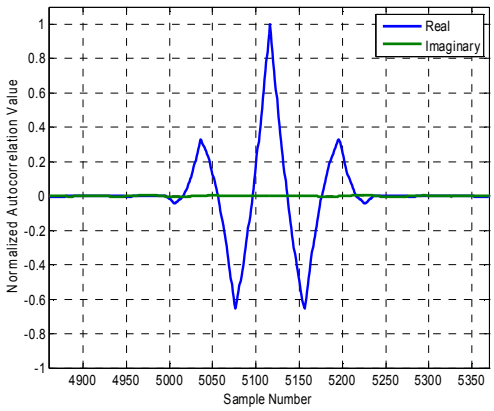

Figure 2 Normalized auto-correlation value of the unfiltered GIOVE-A PRN 51 E5 code with 120 samples per chip and arbitrary chip shift

In order to theoretically analyse the performance of E5 signal acquisition, it is required to have a closed form expression to compute the autocorrelation function. For BOC(*kn,n*) signals, the autocorrelation function of the unfiltered signal is given by [8]

$$R(\tau)=\begin{cases}(-1)^{k+1}\left[\dfrac{1}{p}\left(-k^2+2kp+k-p\right)-(4p-2k+1)\dfrac{|\tau|}{T_c}\right], & |\tau|<T_c\\ 0, & otherwise\end{cases} \quad (1)$$

where $k=\lceil 2p|\tau|/T_c \rceil$ =1.5 and n=10 in case of BOC(15,10). It is interesting to note that despite the similarities in shape, subtle differences exist between BOC(15,10) and AltBOC(15,10) autocorrelation functions. Less work has been reported in the literature concerning the exact expression for the autocorrelation function. However, a very close approximation is provided in [9] as a general expression for Complex Double-Binary-Offset Carrier (CDBOC) modulations. The equation is repeated here for AltBOC signals.

$$R_1(\tau)=\sum_{i=0}^{N_1-1}\sum_{k=0}^{N_2-1}\sum_{i_1=0}^{N_1-1}\sum_{k_1=0}^{N_2-1}(-1)^{i+i_1+k+k_1}\times \Lambda_{T_B}\left(\tau-(i-i1)T_{B_1}-(k-k1)T_{B_{12}}\right) \quad (2a)$$

$$R_2(\tau)=\sum_{l=0}^{N_3-1}\sum_{m=0}^{N_4-1}\sum_{l_1=0}^{N_3-1}\sum_{m_1=0}^{N_4-1}\sum_{p=0}^{N_{res}-1}\sum_{p_1=0}^{N_{res}-1}(-1)^{l+l_1+m+m_1}\times \Lambda_{T_B}\left(\tau-(l-l_1)T_{B_3}-(m-m_1)T_{B_{34}}-(p-p_1)T_{B_{12}}\right) \quad (2b)$$

$$R(\tau)=R_1(\tau)+R_2(\tau) \quad (2)$$

where $N_1=3, N_2=2, N_3=3, N_4=1,$ $T_{B_i}=T_c/N_i$, $T_{B_{ij}}=T_c/(N_i N_j)$, $N_{res}=N_1N_2/(N_3N_4)$, $\Lambda_{T_B}(t)$ is a trianguler pulse of support $2T_{B_{12}}$ and T_c is the chip period of AltBOC(15,10).

Figure 3 shows the auto-correlation function generated with these two methods along with that obtained from ACF of GIOVE-A PRN 51. The corresponding errors are plotted in Figure 4. Note that the ACF generated with the CDBOC expression has less than 5% error whereas the ACF expression of BOC(15,10) has more than 15% deviation to the one obtained with GIOVE-A PRN 51. Since the theoretical evaluation of acquisition performance parameters largely depend on the auto-correlation function, we use equation (2) for our analysis unless otherwise specified.

As noted, the auto-correlation function has side peaks which result in ambiguous signal acquisition. In the next section we discuss several acquisition strategies presented in the literature, addressing this problem.

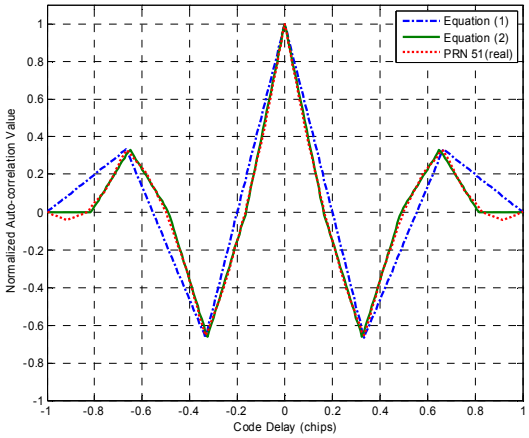

Figure 3 Normalized auto-correlation value generated using equation (1), equation (2) and unfiltered GIOVE-A PRN 51 E5 codes

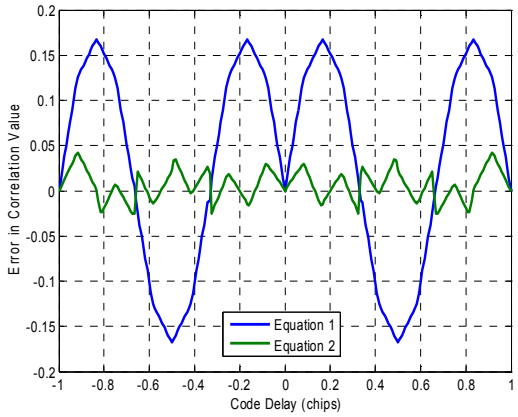

Figure 4 Error in correlation value computed using Equations 1 and 2 with respect to that of GIOVE-A PRN 51

ACQUISITION COMPLEXITY AND THE EFFECT OF CODE SEARCH STEP SIZE

First, the required receiver bandwidth to accommodate the two main lobes of 51.15MHz imposes a limitation on the minimum sampling frequency and is much higher than that required by other GNSS signals. Second, the sharp main peak in the auto correlation function restricts increasing the code search step size as with the case of BOC signals [10]. Third, the side peaks of the auto correlation function cause a threat of false transition to the tracking process although they also give opportunities for detecting the signal. Typical sampling frequencies ≥ 122.76MHz have been used (see [1]) to generate the local replica and to perform the correlation process. Reducing the code search step size increases the number of cells to search during the acquisition and also does not eliminate the side peak problem especially at low signal strengths.

For the AltBOC(15,10) signal, the effect of code search step size on the correlation value is shown in Figure 5.

The best case and the worst case are chosen to obtain an insight into the sharpness of the main peak and the effect of the side peaks. The best case value is the highest maximum correlation that can be obtained for any given code delay. This value always corresponds to the peak of the auto-correlation function. The worst case value is the lowest maximum correlation obtained by stepping through the autocorrelation function with steps of a given size. As an example, for an ideal BPSK auto-correlation triangle, when the search step is 0.5, the best case correlation value is 1 and the worst case value s 0.75 (normalized). For the BPSK case the worst case correlation value follows a linear degradation with increasing step size, as expected with a symmetrical triangular correlation function. For the AltBOC(15,10) case, not only is the degradation more steep, but also there are nulls produced by the regularly spaced autocorrelation nulls between side peaks. A typical code search step size of 0.5 experiences a loss of up to 8.8 dB compared to the best case and up to 6.3 dB loss compared to BPSK correlation waveform with the same search step.

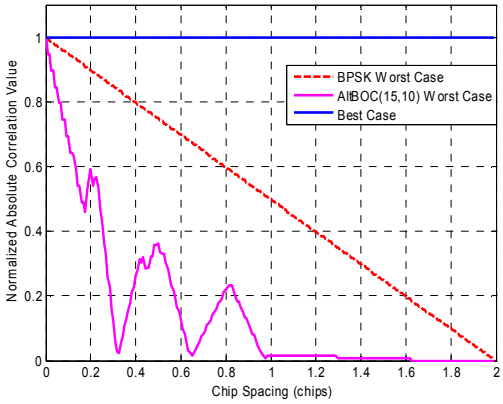

Figure 5 Effect of code search step size on the correlation value; worst case and best case for AltBOC(15,10) and BPSK Auto-correlation waveforms

As an example of calculating the number of search cells, consider a one millisecond pre-detection integration period which is the length of a primary code of E5. For the same worst case correlation loss as the BPSK case of 2.5 dB with a code search step size of 0.5, we need to set the step size to about 0.083 chips for AltBOC(15,10). This results in 10230*(1/0.083) ~= 122760 search cells which is same as the number of samples in one millisecond assuming a typical sampling frequency of 122.76 MHz. Alternatively, one can decide to use a search step of 0.5 and 6 dB loss can be regained by increasing the pre-detection coherent integration time by four times which results in a total of 10230*(1/0.5)*4 = 81840 cell searches. With the latter approach we require a finer search of the code delay for a smooth and unambiguous transition to the tracking process. The finer search involves cells corresponding to only 2 chips ambiguity (24 cells). However, increasing the coherent integration duration decreases the Doppler bin size and this inturn increases the number of frequency cells to

search. In effect, the total search time increases sixteen fold.

Note that this approach holds good for any BOC signal and each BOC signal would have a particular value of code search step size away from zero that has acceptable correlation loss (like 0.5 step size and 6.3dB for AltBOC(15,10)). However at low received signal strengths this approach might not always perform well due to noise. Thus the code search step size plays an important role in determining the probability of detection and the acquisition time. Throughout the paper we consider only the search dimension along the time axis. The analyses do not consider Doppler because the methodologies discussed in this paper do not directly relate to Doppler search, but it has to be borne in mind that increasing the integration time increases the number of frequency cells to search.

Several methods have been proposed in the literature to address the problem of sharp main peak and side peak ambiguity which a receiver experiences during acquisition of E5 signals. These methods can be broadly classified as search strategy based and correlation scheme based techniques.

SEARCH STRATEGY BASED TECHNIQUES FOR ACQUISITION

Because of the split spectrum properties of AltBOC signals, individual signals can be acquired by independently processing the main lobes. Different acquisition approaches have been studied in [1, 11].

(1) Single Side-Band Acquisition (SSB)
   i. E5a-Q only or E5b-Q only
   ii. {E5a-Q, E5a-I} or {E5b-Q, E5b-I}
(2) Double Side-Band Acquisition (DSB)
   i. E5a-Q and E5b-Q
   ii. Non coherent combination of {E5a-Q, E5a-I} and {E5b-Q, E5b-I}
(3) Full-band Independent Code Acquisition (FIC)
   i. Any of the E5a-Q, E5b-Q, E5a-I and E5b-I
   ii. Coherent combination of {E5a-Q, E5b-Q} or {E5a-I, E5b-I}
   iii. Non coherent combination of I channels and Q channels of ii)
   iv. Non coherent combination of E5a channel and E5b channel
(4) Direct AltBOC Acquisition
   i. 8-PSK like processing

A brief summary of the earlier study will be presented here (for details with block diagrams see [1, 11]). In the SSB approach, one of the main lobes, either E5a or E5b, is filtered with a 20.46 MHz filter and then correlated with respective codes (no sub-carrier is required). This results in a BPSK(10) like correlation triangle. In the DSB approach, both the E5a and E5b lobes are filtered, correlated with respective codes and combined. Again, this results in a BPSK(10) like correlation triangle.

In the Full-band Independent Code Acquisition method, a locally generated individual code with corresponding sub-carrier is multiplied with the received signal without filtering (i.e. no filter apart from the RF front-end filter). This is possible because each of the codes used in E5 is quasi-orthogonal to the other. Note that each individual code correlation result is complex and can be combined coherently or non-coherently with the results of other codes. Even though the magnitude of individual correlation values is a BPSK(10) like correlation triangle, coherent combination of pilot-only or data-only channels yields correlation waveform similar to AltBOC(15,10). However, the combination of E5a and E5b channels results in a BPSK(10) like correlation triangle as with the case of DSB. Figure 6 shows the correlation waveforms for some of the approaches mentioned above.

The difference between SSB or DSB and the FIC method is the frequency of operation of the correlation circuit. Although the side-band filtering overhead is removed in FIC, there is no scope for down sampling and the correlator circuit should operate at the original sampling frequency.

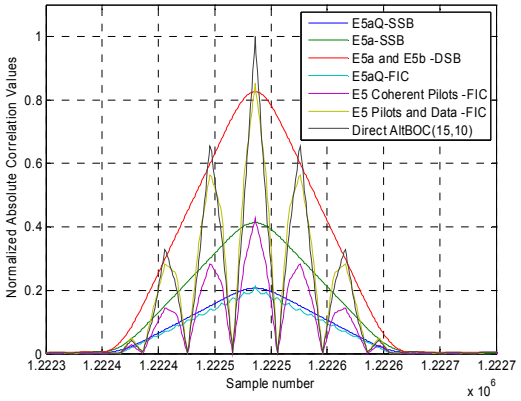

Figure 6 Normalized Absolute correlation values for different search strategies using GIOVE-A PRN 51; Side bands are filtered with a filter of bandwidth 20.46MHz

The Direct AltBOC Acquisition method makes use of the 8-PSK principle and the local replica can be generated using a look-up table method [5,6]. Note that even though the correlator circuit operates at the original sampling frequency, it is not required to generate the individual sub-carriers to combine with the individual codes as the look-up table is easy to realize.

Finally it is worth mentioning that among all the four approaches only the Direct AltBOC approach provides the complete received power. Even though the DSB and FIC approaches accommodate all the four codes, they forego the 15% power contained in the product codes [5,6] (also observe in Figure 6). Table 1 summarizes the search strategy based acquisition approaches discussed so far. We use the term extra filter because to take advantage of the AltBOC modulation, the tracking process requires a 51 MHz front end filter and hence whatever we are going to use in the acquisition is an extra filter for the receiver.

		Extra Filter Required?	Down sampling Possible?	Code / Subcarrier Generators	Shape of the Correlation Waveform	Correlation Power(% of Direct-AltBOC)
SSB	Any One Code	Yes (one)	Yes	1 Code	BPSK(10)	21
	One Side-band	Yes (one)	Yes	2 Code	BPSK(10)	42
DSB, Both side Bands		Yes (two)	Yes	4 Code	BPSK(10)	84
FIC	Any One Code	No	No	1 Code, 1 Complex Sub-carrier	BPSK(10)	21
	Coherent Pilots	No	No	2 Code, 2 Complex Sub-carriers	AltBOC(15,10)	42
	Coherent Pilots & Data	No	No	4 Code, 2 Complex Sub-carriers	AltBOC(15,10)	84
Direct AltBOC		No	No	4 Code, one 16x8 Lookup table	AltBOC(15,10)	100

Table 1 Summary of the search strategy based schemes

Acquisition schemes use the search strategy based techniques to reduce the number of cells and hence to reduce the mean acquisition time $\overline{T_{acq}}$. For example in [1] a multi-resolution approach to find the code delay is demonstrated. First the coarse acquisition is done using the SSB strategy with one pilot code. With this the acquisition engine can search at 0.5 chips with a total of 20460 cells for a one millisecond pre-detection integration. As a second step, fine estimate of the code delay is performed with code search step size of $1/12$ over 2 chips covering 24 cells. This reduces the total number of cells searched and also avoids the side peak ambiguity. However note that the first phase estimate is going to incur a loss of more than 6 dB in P_d (because of only 21% power) compared to the Direct AltBOC processing. In order to compensate for this loss a minimum of four millisecond pre-detection integration time is required which brings up the number of search cells to 81920.

CORRELATION SCHEME BASED TECHNIQUES FOR ACQUISITION

Another class of acquisition technique proposed in the literature addresses the problem of side peak ambiguity in BOC signals [2, 3]. These techniques concentrate on the correlation function and try to synthesize a correlation waveform void of any strong side peaks. Most of these techniques are designed keeping the tracking process also in mind and hence these techniques hardly address the correlation loss and P_d for larger code search step size scenarios. Some of the related techniques are as follows. Again, we briefly discuss the applicability of these methods.

(1) 'BPSK-like' method proposed in [12] and modified in [3]
(2) Sub Carrier Phase Cancellation Method (SCPC) proposed in [2]
(3) Very Early + Prompt ($|VE^2+P^2|$) method mentioned in [2]

The 'BPSK-like' method essentially falls into the SSB/DSB approach discussed in the previous section.

The SCPC method is based on the idea of removing the sub-carrier from the received signal (after carrier removal). In this method, the complex local replica is generated as in equation (3) where $r(t)$ is the local replica, $c(t)$ is the local code, $sc(t)$ is the local sub-carrier and T_{sc} is the sub-carrier period.

$$\begin{aligned} r_I(t-\hat{\tau}) &= c(t-\hat{\tau}).sc_I(t-\hat{\tau}) \\ &= c(t-\hat{\tau}).sc(t-\hat{\tau}) \end{aligned} \tag{3a}$$

$$\begin{aligned} r_Q(t-\hat{\tau}) &= c(t-\hat{\tau}).sc_Q(t-\hat{\tau}) \\ &= c(t-\hat{\tau}).sc\left(t-\hat{\tau}-\frac{T_{sc}}{4}\right) \end{aligned} \tag{3b}$$

$$r(t-\hat{\tau}) = c(t-\hat{\tau}).\left(sc(t-\hat{\tau}) + i \times sc\left(t-\hat{\tau}-\frac{T_{sc}}{4}\right)\right) \tag{3}$$

As seen from the equation, the sub-carrier in the quadrature arm of the local replica is phase-shifted by one quarter of the sub-carrier period. It turns out that when the BOC signal is multiplied with this local replica the shape of the correlation function is similar to the BPSK triangle.

At this juncture, it is interesting to note that this is exactly the principle used to combine four codes in AltBOC modulation scheme (see the AltBOC modulation equations in [5, 6]). The correlation process FIC approach works on the basis of the SCPC method. Figure 7 shows the E5a-Q correlation waveform. We can conclude that the SCPC method is not directly applicable to process the complete AltBOC signal since all the orthogonal components of the sub-carrier and the carrier have already been used to combine the four codes.

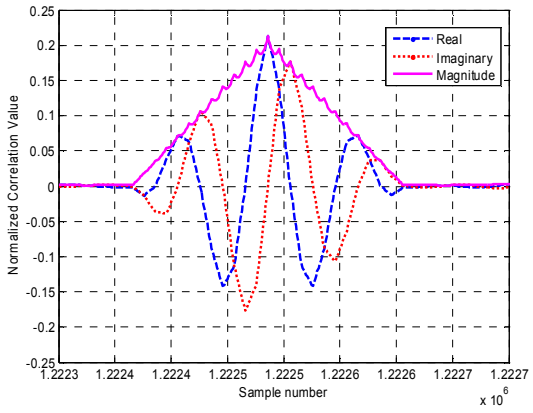

Figure 7 Normalized Correlation value for E5a-Q code of GIOVE-A PRN 51

The $|VE^2+P^2|$ method works on the basis that if magnitudes of two correlation values of the BOC signal separated by an appropriate delay are combined, then it results in a correlation waveform whose shape is similar to the BPSK triangle. In the $|VE^2+P^2|$ method the local replica is generated as follows [2].

$$r_P(t-\hat{\tau}) = c(t-\hat{\tau}).sc(t-\hat{\tau}) \quad (4a)$$

$$r_{VE}(t-\hat{\tau}) = c\left(t-\hat{\tau}-\frac{T_{sc}}{4}\right).sc\left(t-\hat{\tau}-\frac{T_{sc}}{4}\right) \quad (4b)$$

For AltBOC(15,10) signal, the delay is 0.167 chips. The resulting correlation waveform with this method is shown in Figure 8. Observe that the shape is similar to BPSK triangle and also the peak is flat across 0.167 chips. The bias in the centre of the resulting correlation waveform can be easily compensated as it is a known value.

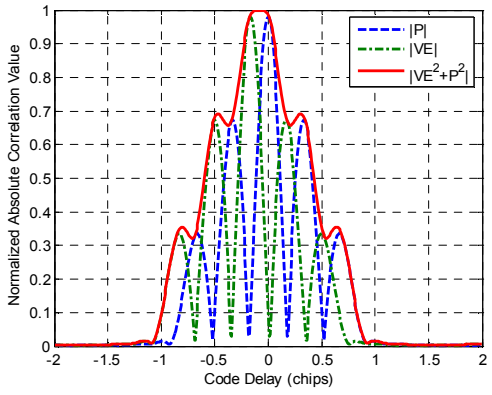

Figure 8 $|VE^2+P^2|$ method for AltBOC(15,10)

We now draw attention to the principles behind the $|VE^2+P^2|$ method. The problem of reduced P_d with increasing code search step size has been studied earlier for CDMA systems. The problem which exists in BOC modulated signals is not totally different from this. Even for the BPSK signals, an increase in the step size reduces the probability of detection. Also there is an issue of residual code phase offset (i.e. the point where the receiver starts the correlation may not be aligned with the correlation peak and there can be an initial ambiguity of up to one step size) which brings in the best and worst case scenarios. In [4] this problem is addressed in detail and as a solution a method of addition of successive correlation samples is proposed. For BPSK, this method flattens the correlation function around the peak and hence increases the P_d and also makes the correlation function less sensitive to the residual code phase offset. The $|VE^2+P^2|$ method used for BOC signals is a special case of this successive correlation samples addition method. The delay between the samples that are combined is controlled so as to obtain a BPSK like correlation triangle.

We will now analyse the effect of code search step size with the $|VE^2+P^2|$ method, see Figure 9. The worst case correlation values for the $|VE^2+P^2|$ method are close to that of BPSK worst case values and swings around it. For example in order to obtain the losses similar to 0.5 step sizes of BPSK, we should use 0.4 step size for the $|VE^2+P^2|$ method. For 0.5 step size we incur only about 1 dB loss compared to BPSK worst case. A keen observation of the $|VE^2+P^2|$ worst case loss curve shows us an interesting phenomenon. The curve shows flattened response at three places. The middle one is worth closely observing. From 0.5 to around 0.8 step size, the correlation loss remains at 0.67. This means that even at 0.8 step size we will incur only a loss of 3.5 dB and this loss is less than even the BPSK worst case at 0.8 step size.

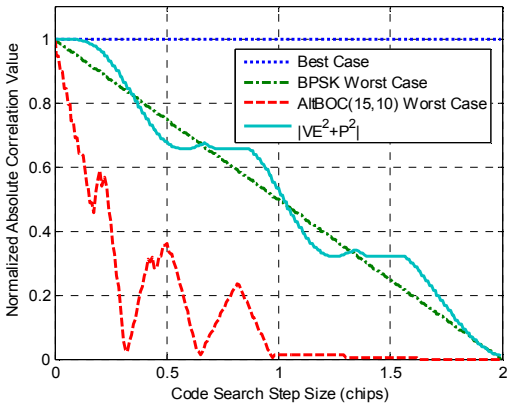

Figure 9 Effect of code search step size on the correlation values including $|VE^2+P^2|$ method

To understand the advantage in terms of number of cell searches we again consider a one millisecond pre-detection integration period. With 0.8 step size, we need only 10230*(1/0.8) = 12788 cells in the first step and around 36 cells (assuming 3 chip ambiguity and 1/12 chip step) in the second step. This is a huge reduction in the number of cells to search for the acquisition (which requires 0.1 chip step for the same loss with Direct AltBOC). When compared to the 0.5 chip stepping case which requires 20460 cell searches, we obtain an improvement of about 37%.

The above analysis did not consider the effect of noise and the effect of RF front-end filtering. In practice whenever we add two signal components, we will also be adding the noise components and the results slightly degrade at lower received signal strengths. Nevertheless the advantage of this method is sufficient to overcome the degradation due to noise as we will see when we evaluate P_d and $\overline{T_{acq}}$. When the received signal is filtered, the correlation functions will no more be sharp and hence the delay value of 0.167 chips may not be valid. But without loss of generality we can say that an optimum delay can be found for the particular filter used in a receiver to make use of the $|VE^2+P^2|$ method.

SYSTEM DESCRIPTION

In this section we describe the acquisition engine architecture to realize the Direct AltBOC acquisition and the $|VE^2+P^2|$ methods. Figure 10 shows the Direct AltBOC acquisition architecture. Δ is the code search step size used for stepping the energy search. As discussed earlier this value is typically 0.083 chips. Once the decision is made, the control is handed over directly to the tracking process.

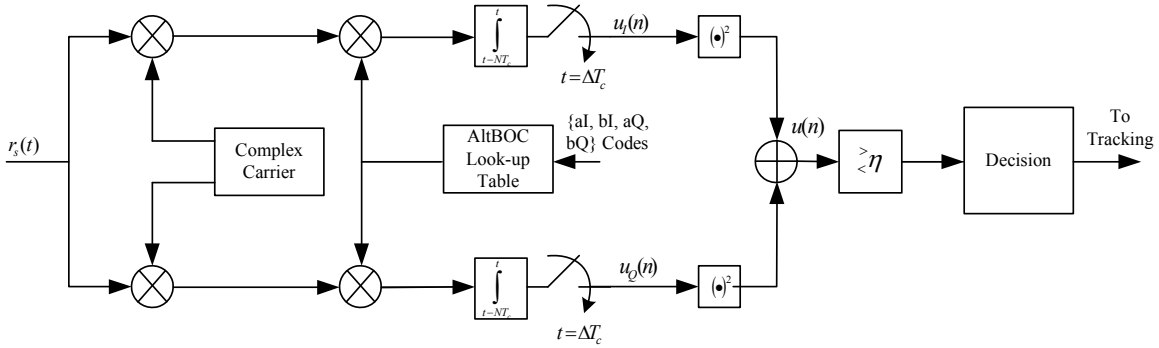

Figure 10 Direct AltBOC Acquisition Architecture

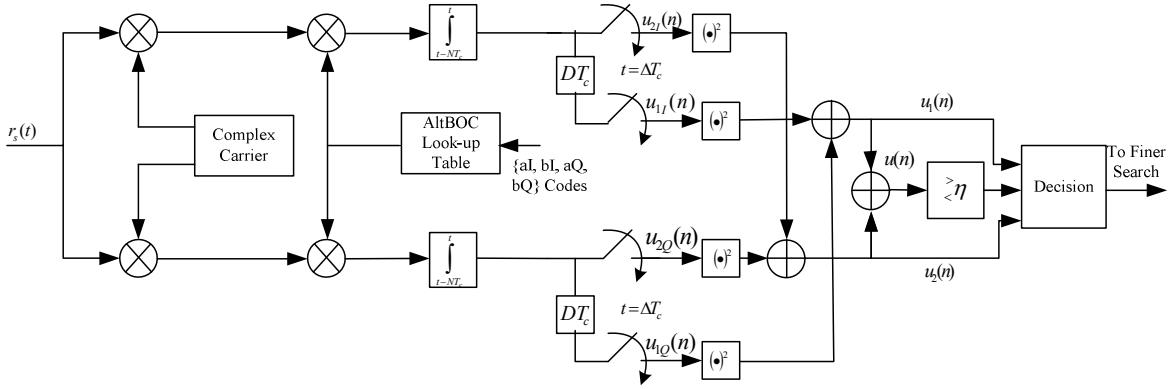

Figure 11 Direct AltBOC Acquisition Architecture with $|VE^2+P^2|$ method; Specific sampling frequency

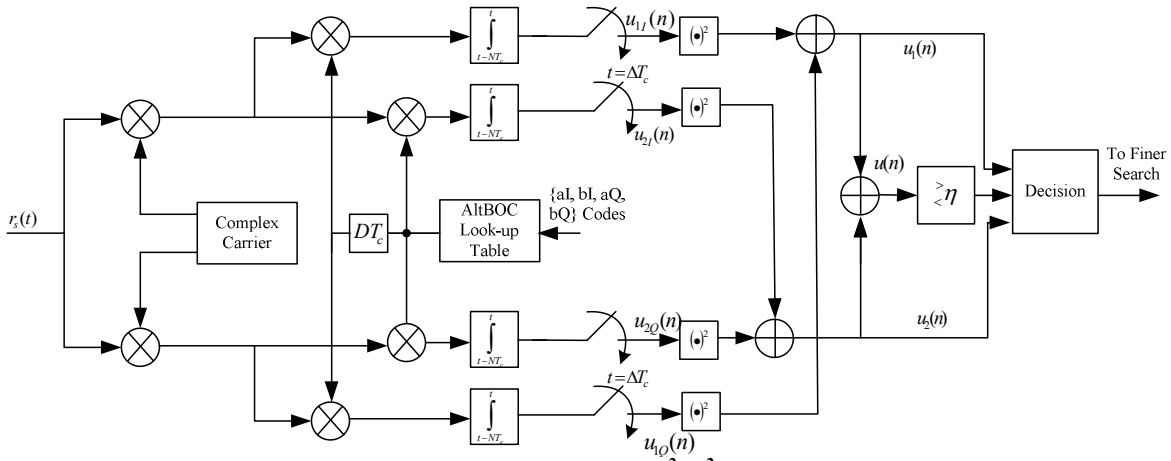

Figure 12 Direct AltBOC Acquisition Architecture with $|VE^2+P^2|$; Arbitrary (Valid) sampling frequency

Figure 11 shows the architecture with addition of VE and P correlation values when the sampling frequency is such that it enables us to provide the required code delay D between the samples used for the addition. This is the case with sampling frequency of 122.76 MHz which can be used to realize the required D = 0.167 chips (every alternate sample). Observe that the architecture does not use any additional correlators compared to the previous approach. In practice it may not be possible for the designer to realize this delay from the sampling interval due to RF filtering effects or other hardware limitations.

Figure 12 shows the architecture of the $|VE^2+P^2|$ method for the case where the required delay D is difficult to realize using the sampling frequency. Here the output of the AltBOC look-up table is delayed by a value DT_c and separate channels are used for correlation. This increases the number of correlators required but the advantage is that it can be used for any arbitrary (but valid) sampling frequency. A couple of points should be noted regarding the architecture. All the lines after the carrier mixing stage carry complex values. In Figure 11 and Figure 12 Δ can be as large as 0.8 as discussed earlier. Also with these two architectures, the control is transferred to a finer code delay search instead of tracking. For the finer code delay search, the same architecture can be used, by switching off the appropriate correlators.

Now we discuss the decision statistic. A simple hypothesis testing with a threshold η can be employed by comparing the output of the correlator $u(n)$ with η and a decision can be made to enter the finer search process. By making use of the individual correlation outputs in the case of $|VE^2+P^2|$ method one can estimate the code phase more accurately and select this good estimate instead of randomly selecting either VE or P. For example the values of $u(n)$, $u_1(n)$ and $u_2(n)$ and the difference between $u_1(n)$ and $u_2(n)$ can approximately tell us where we are from the main peak. We will not go into the sophisticated algorithms but only use the simple hypothsis testing to compute the probability of detection.

PROBABILITY OF DETECTION AND MEAN ACQUISITION TIME EVALUATION

In this section, the probability of detection is evaluated for the acquisition strategies described so far and also the mean acquisition time is evaluated for Direct AltBOC and $|VE^2+P^2|$ methods. For the sake of simplicity we will consider both the architectures in Figure 11 and Figure 12 to be the same in our analysis, without loss of generality.

The decision statistic for the Direct AltBOC architecture is given by

$$u(n) = u_I{}^2(n) + u_Q{}^2(n) \tag{5}$$

Along with the signal components, the output of both the I and the Q channels $u_I(n)$ and $u_Q(n)$ contain noise components $n_I(n)$ and $n_Q(n)$ and are assumed to be statistically independent, zero mean, Gaussian distributed.

Also the signal components in the I and Q channels are assumed to be independent Gaussian distributed random variables with mean m_I and m_Q respectively and equal variance of σ^2. It has been shown [13] that the sum of squares of M independent Gaussian random variables of the same variance is non-centrally distributed with M degrees of freedom and with non-centrality parameter λ .

The non-centrality parameter is given by

$$\lambda^2 = \sum_{i=1}^{M} m_i{}^2 \tag{6}$$

For the Direct AltBOC case, under the hypothesis H_0 when there is no signal present, the decision statistic has a central chi-square distribution with 2 degrees of freedom with PDF $p_n(x)$ and the Probability of False Alarm P_{fa} is then given by

$$P_{fa} = \int_{\eta}^{\infty} p_n(x)dx = e^{\frac{-\eta}{2\sigma^2}} \tag{7}$$

Under the hypothesis H_1 when the signal is present the decision statistic has a non-central chi-square distribution with 2 degrees of freedom with PDF $p_s(x)$ and the non-centrality parameter $\lambda^2 = m_I{}^2 + m_Q{}^2$. The Probability of detection is then given by

$$P_d = \int_{\eta}^{\infty} p_s(x)dx \tag{8}$$

The decision statistic for the $|VE^2+P^2|$ architecture is given by

$$\begin{aligned} u(n) &= u_1{}^2(n) + u_2{}^2(n) \\ &= u_{1I}{}^2(n) + u_{1Q}{}^2(n) + u_{2I}{}^2(n) + u_{2Q}{}^2(n) \end{aligned} \tag{9}$$

Again assuming the Gaussian distribution and statistical independence of the individual correlation outputs we can compute the detection and false alarm probabilities.

Under the hypothesis H_0 when there is no signal present, the decision statistic has a central chi-square distribution with 4 degrees of freedom and P_{fa} can is along the similar lines as equation (7).

Under the hypothesis H_1 when the signal is present the decision statistic has a non-central chi-square distribution with 4 degrees of freedom with PDF $p_s(x)$ and the non-centrality parameter $\lambda^2 = m_{1I}{}^2 + m_{1Q}{}^2 + m_{2I}{}^2 + m_{2Q}{}^2$ and the Probability of detection is given by equation (8).

In both the methods, we can perform a non-coherent integration of the decision statistic to improve the sensitivity and correspondingly the degree of freedom

parameter of the chi-square distributions will have to be multiplied by the number of non-coherent summations.

In order to compute the probabilities, first the threshold η for a chosen P_{fa} is computed by numerically evaluating the inverse chi-square distribution. Then the P_d is computed using the η with the help of the CDF of chi-square distribution [14]. In our analysis and simulations for the comparison we consider a P_{fa} of 10^{-3} and a pre-detection coherent integration time of 1 millisecond.

Using the probabilities of detection for different received signal strengths and probability of false alarm, the mean acquisition time is evaluated. Assuming a single dwell search the mean acquisition time is given by [15]

$$\overline{T_{acq}} = \frac{2 + (2 - P_d)(N_t - 1)(1 + k_p P_{fa})}{2P_d} T_{coh} N_{nc} \qquad (10)$$

where N_t is the size of the uncertainty region, k_p is the penalty due to falsle alarm, T_{coh} is the pre-detection coherent integration duration and N_{nc} is the number of non-coherent summations. Note that in practice, the penalty due to false alarm will be comparitively less in the case of $|VE^2+P^2|$ method as we will be entering the finer code delay search process and not the tracking process. The following figures show the comparision of P_d and $\overline{T_{acq}}$. For the approaches with a two step search process, only the coarse (initial) step is considered as it is the dominant part.

Figure 13 shows the worst case probability of detection for BPSK and AltBOC. To show the step size required to achieve BPSK like correlation losses and to show the effect of larger step size, $\Delta = 0.083$ as well as $\Delta = 0.5$ are chosen for AltBOC. Note that a loss of 6.3 dB between AltBOC with $\Delta = 0.5$ and BPSK $\Delta = 0.5$ (or AltBOC $\Delta = 0.083$) can be read from the graph.

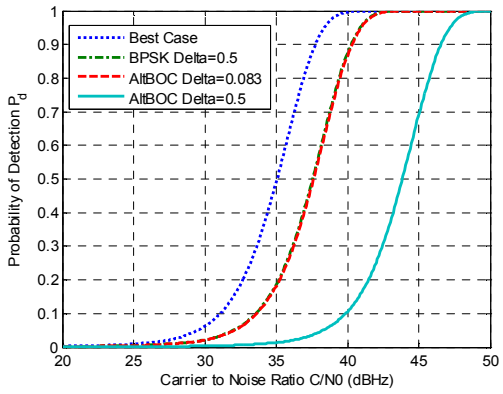

Figure 13 Worst case probability of detection for BPSK and AltBOC

Figure 14 shows the average probability of detection for BPSK and AltBOC with Δ as in Figure 13. The average correlation loss scenario stems from the fact that we will not always encounter the worst case and residual code phase offset will have a uniform distribution in $[0, \Delta)$. Note that the difference between AltBOC $\Delta = 0.5$ and the BPSK $\Delta = 0.5$ reduces to around 2.2 dB in this case.

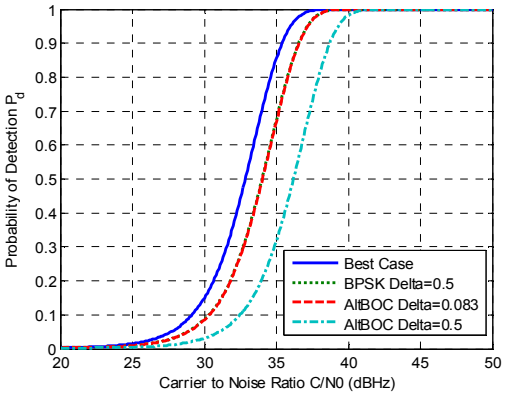

Figure 14 Average probability of detection for BPSK and AltBOC

Figure 15 provides the average probability of detection for the acquisition approaches considered in Figure 6. Note that the difference in the power distribution among different approaches is evident with the probability of detection curve.

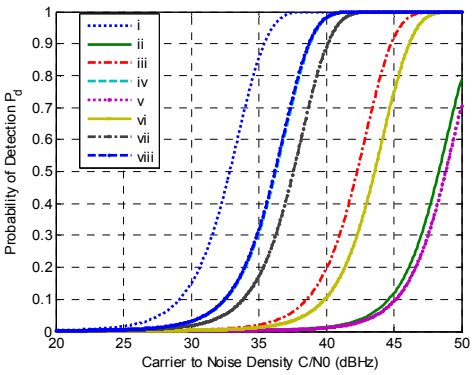

Figure 15 Average probability of detection for different cases (Legend : i. Best Case, ii. E5aQ-SSB, iii. E5a-SSB, iv. E5a and E5b – DSB, v. E5aQ-FIC, vi. E5 Pilots – FIC, vii. E5 Pilots and Data FIC, viii. Direct AltBOC)

Figures 16 and 17 provide the theoretical and simulated average and worst case probability of detection for the $|VE^2+P^2|$ method with both $\Delta = 0.5$ and 0.8 scenarios. In figure 16 we can see that the average probability of detection for the $|VE^2+P^2|$ method is worse by 0.4 dB compared to the BPSK case and the $|VE^2+P^2|$ method outperforms Direct AltBOC approach by about 2.2 dB. Figure 17 shows that the worst case loss in the case of $|VE^2+P^2|$ method is only 1 dB worse than that of the BPSK method and has an improvement of 5.3 dB compared to the Direct AltBOC approach.

Legends for Figures 16 through 19: i. BPSK theoretical, ii. AltBOC Δ =0.5 theoretical, iii. $|VE^2+P^2|$ Δ =0.5 theoretical, iv. $|VE^2+P^2|$ Δ =0.8 theoretical, v. BPSK simulation, vi. AltBOC Δ =0.5 simulation, vii. $|VE^2+P^2|$ Δ =0.5 simulation, viii. $|VE^2+P^2|$ Δ =0.8 simulation.

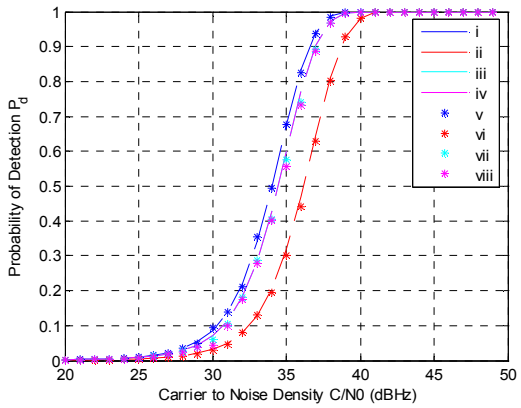

Figure 16 Average probability of detection for AltBOC and $|VE^2+P^2|$ methods (- - :Theoritical, * : Simulation)

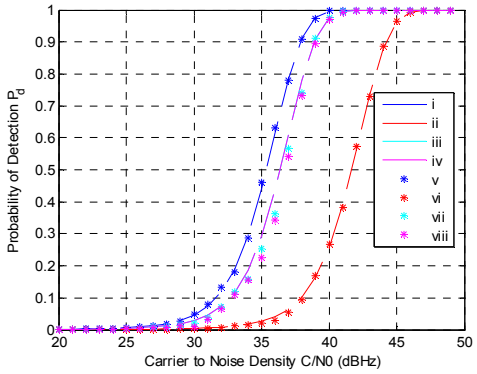

Figure 17 Worst case probability of detection for AltBOC and $|VE^2+P^2|$ methods(- - :Theoritical, * : Simulation)

In Figure 18 and Figure 19 we compare the mean acquisition time for the probability of detection scenarios considered in Figure 16 and Figure 17. The simulated values match the theoretical values except at lower C/N0 values. Observe that the $|VE^2+P^2|$ method with Δ =0.8 chip step performs better than the BPSK case with Δ =0.5 at a given C/N0.

CONCLUSION

In this paper we discussed the complexity and problems with the Galileo E5 signal acquisition and revisited different strategies which address these problems. We analysed the probability of detection and the mean acquisition time for these strategies especially concentrating on the $|VE^2+P^2|$ method along with the acquisition engine architecture. For the same probability

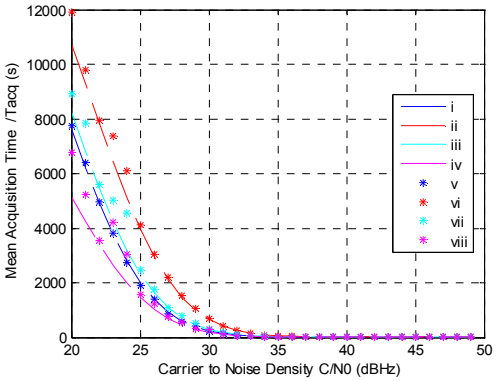

Figure 18 Mean Acquisition time for the Average probability of detection scenario (- - :Theoritical, * : Simulation)

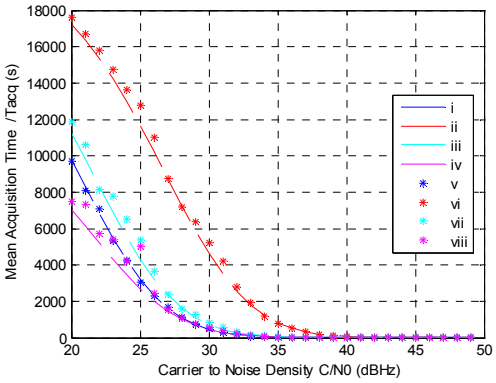

Figure 19 Mean Acquisition time for the worst case probability of detection scenario (- - :Theoritical, * : Simulation)

of detection, compared to the Direct AltBOC approach, the $|VE^2+P^2|$ method results in an improvement in C/N0 of about 2.2 dB in the average scenario and about 5.3 dB in the worst case scenario. In addition an interesting observation shows that the correlation loss in $|VE^2+P^2|$ method remains constant for chip step sizes from 0.5 to 0.8 which reduces the mean acquisition time by 37%. We conclude that $|VE^2+P^2|$ method is a good candidate for implementation in Galileo E5 receivers.

ACKNOWLEDGEMENTS

The authors would like to acknowledge that this research work has been carried out under the Australian Research Council (ARC) project DP0556848.

REFERENCES

[1]. Dovis F., Mulassano P., Margaria D., "Multiresolution Acquisition Engine Tailored to the Galileo AltBOC Signals", in *Proceedings of ION GNSS 2007*, September 2007.

[2]. Heiries V., Roviras D., Ries L., Calmettes V., "Analysis of Non Ambiguous BOC Signal Acquisition Performance", *Proceedings of ION GNSS 2004*, September 2004.
[3]. Burian A., Lohan E.S., Renfors M., "BPSK-like Methods for Hybrid-Search Acquisition of Galileo Signals", *IEEE ICC'06*, June 2006.
[4]. Yoon S., Song I., Kim S.Y., Park S.R., "A DS-CDMA Code Acquisition Scheme Robust to Residual Code Phase Offset Variation", *IEEE Trans. on Vehicular Technology, Vol. 49, No.6,* November 2000.
[5]. Galileo Open Service Signal-In-Space Interface Control Document, GAL OS SIS ICD/D.0, Draft 0, May 23, 2006.
[6]. GIOVE-A Navigation Signal-In-Space Interface Control Document, Issue 1, Revision 0, 02-03-2007.
[7]. P.Ward, J.W. Betz and C.J. Hegarty, "Satellite Signal Acquisition, Tracking and Data Demodulation", in *Understanding GPS: Principles and Applications,* Second Edition, E.D. Kaplan and C.J. Hegarty, Artech House, Norwood, MA, 2006.
[8]. F.D. Nunes, F.M.G. Sousa, Jose M. N. Leitao "Gating functions for Multipath mitigation in BOC Signals", *IEEE Transactions on Aerospace and Electronic Systems*, Vol 43., No. 3, July 2007.
[9]. E.S. Lohan, A. Lakhzouri and M. Renfors, "Complex Double-Binary-Offset-Carrier Moculation for Unitary Characterization of Galileo and GPS Signals", in *IEE Proceedings – Radar, Sonar and Navigation,* Vol. 53, No. 5, Octobr 2006.
[10]. W. De Wilde, J.-M. Sleewaegen, A. Simsky, C. Vandewiele, E. Peeters, J. Grauwen, and F. Boon, "Fast signal Acquisition technology for new GPS/Galileo Receivers" in *IEEE PLANS* 2006.
[11]. J.-M. Sleewaegaen, W. De Wilde, and M. Hollreiser, "Galileo AltBOC Receiver", in *Proceedings of ENC GNSS 2004*, Rotterdam, Holland, May 16-19, 2004.
[12]. N. Martin, V. Leblond, G. Guilliotel, and V. Heiries, "BOC(x,y) Signal Acquisition Techniques and Performances", in *Proceedings of ION GPS/GNSS 2003,* Portland, OR, September 9-12, 2003.
[13]. R.L. Peterson, D.E. Borth, R.E. Ziemer, An Introduction to Spread Spectrum Communications, 1st edition, Prentice Hall, Upper Saddle River NJ, USA, 1995.
[14]. David. A. Shnidman, "The Calculation of the Probability of Detection and the Generalized Marcum Q Function", *IEEE Transaction on Information Theory*, Vol. 35, No. 2, March 1989
[15]. Jack K Holmes, Coherent Spread Spectrum Systems, Wiley, 1982.